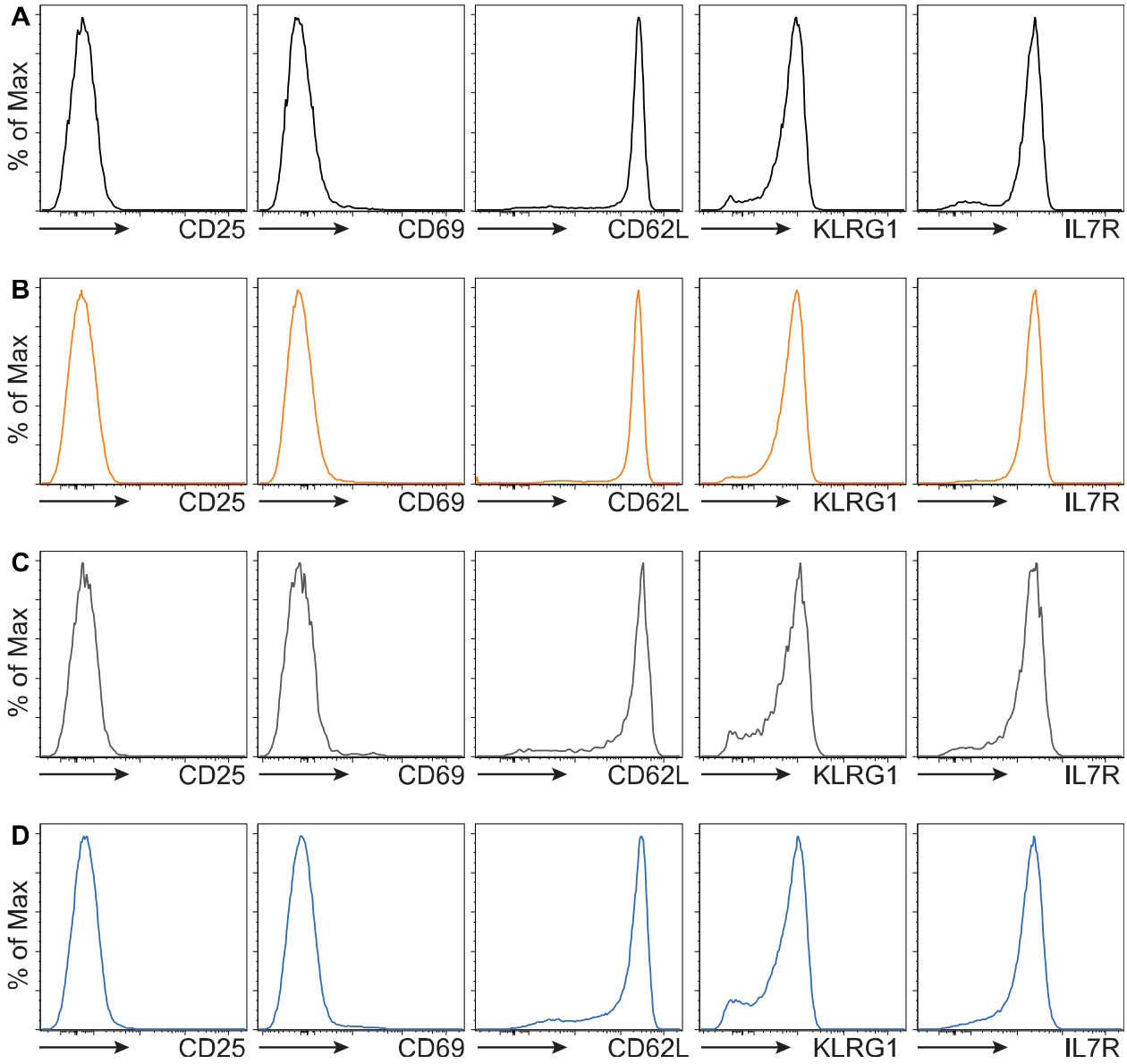

Figure S1 Adult and neonatal CD8+ T cells have equivalent phenotypes before and after selection. Representative histograms show expression of IL2RA/CD25 (associated with activation), CD69 (associated with activation), SELL/CD62L (marker of lymph homing), KLRG1 (marker of SLECs), and IL7R (marker of MPECs) in naive CD8+ cells from (A) adults pre-selection, (B) adults post-selection, (C) neonates pre-selection, and (D) neonates post-selection.

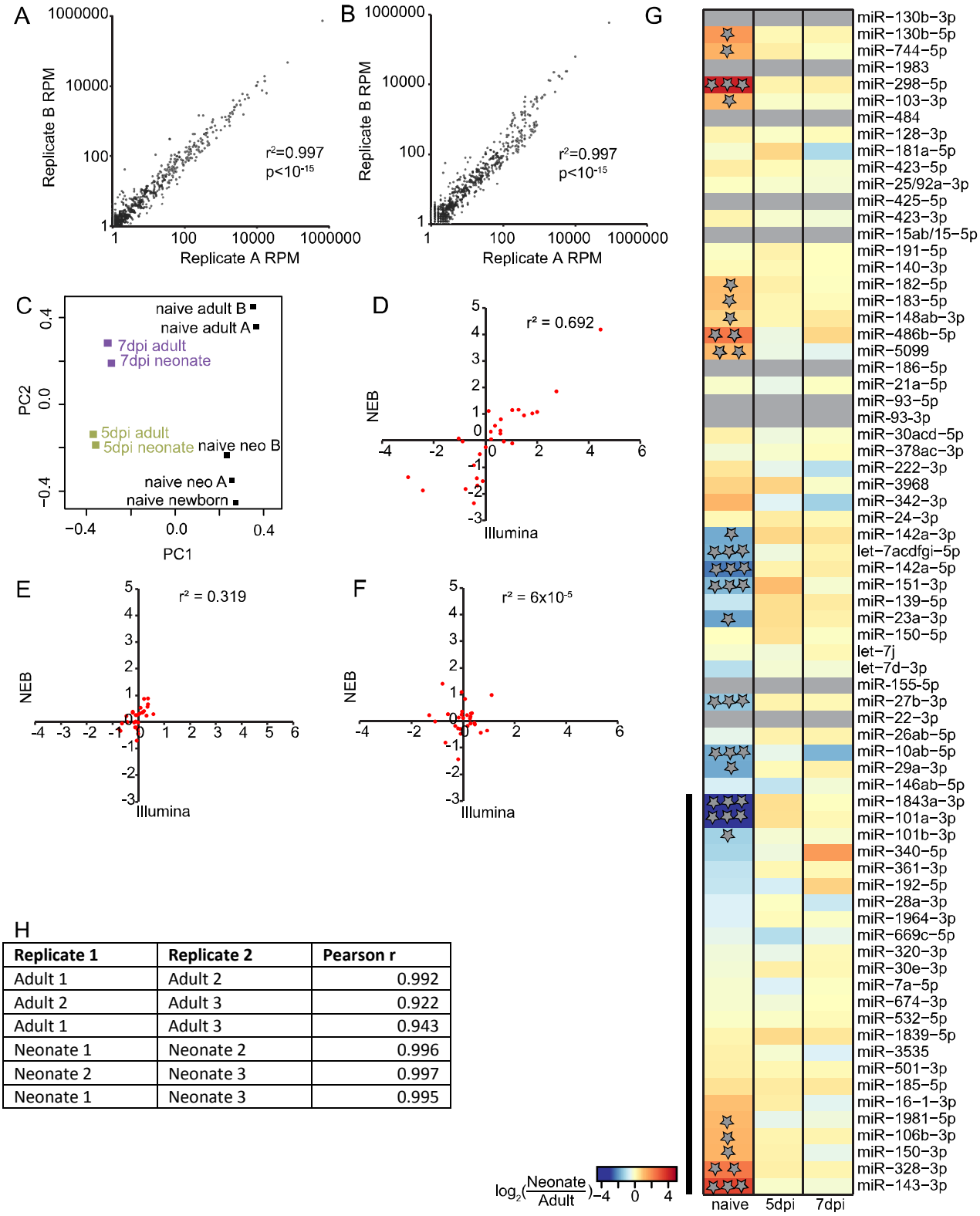

H

Replicate 1	Replicate 2	Pearson r
Adult 1	Adult 2	0.992
Adult 2	Adult 3	0.922
Adult 1	Adult 3	0.943
Neonate 1	Neonate 2	0.996
Neonate 2	Neonate 3	0.997
Neonate 1	Neonate 3	0.995

Figure S2 Differences in miRNA expression are conserved in biological replicates and robust to alterative sequencing protocols. (A and B) Correlation of miRNA expression between two mouse naive CD8+ T cell biological replicates. The reads per million (RPM) of all miRNAs with at least one read are shown for adult (A) and neonatal (B) samples. (C) Principal component analysis on all replicate samples for miRNA sequencing. (D-F) Correlation of miRNA neonatal:adult fold-change values for miRNA sequencing libraries derived from Illumina TruSeq and NEBNext protocols in naive (D), 5-dpi (E), and 7-dpi (F) cells. (G) Heatmap of neonatal:adult fold-change for miRNAs sequenced using the NEBNext protocol. miRNAs marked with a black bar are miRNAs that were captured by the TruSeq protocol, and miRNAs in gray are ones that were not captured by the NEBNext protocol. Differential expression was determined by edgeR. *=$p<0.05$, **=$p<0.005$, ***=$p<0.0005$. (H) Pearson correlation coefficients for all pairwise combinations of human biological replicates, based on miRNAs with at least one read in one of the samples.

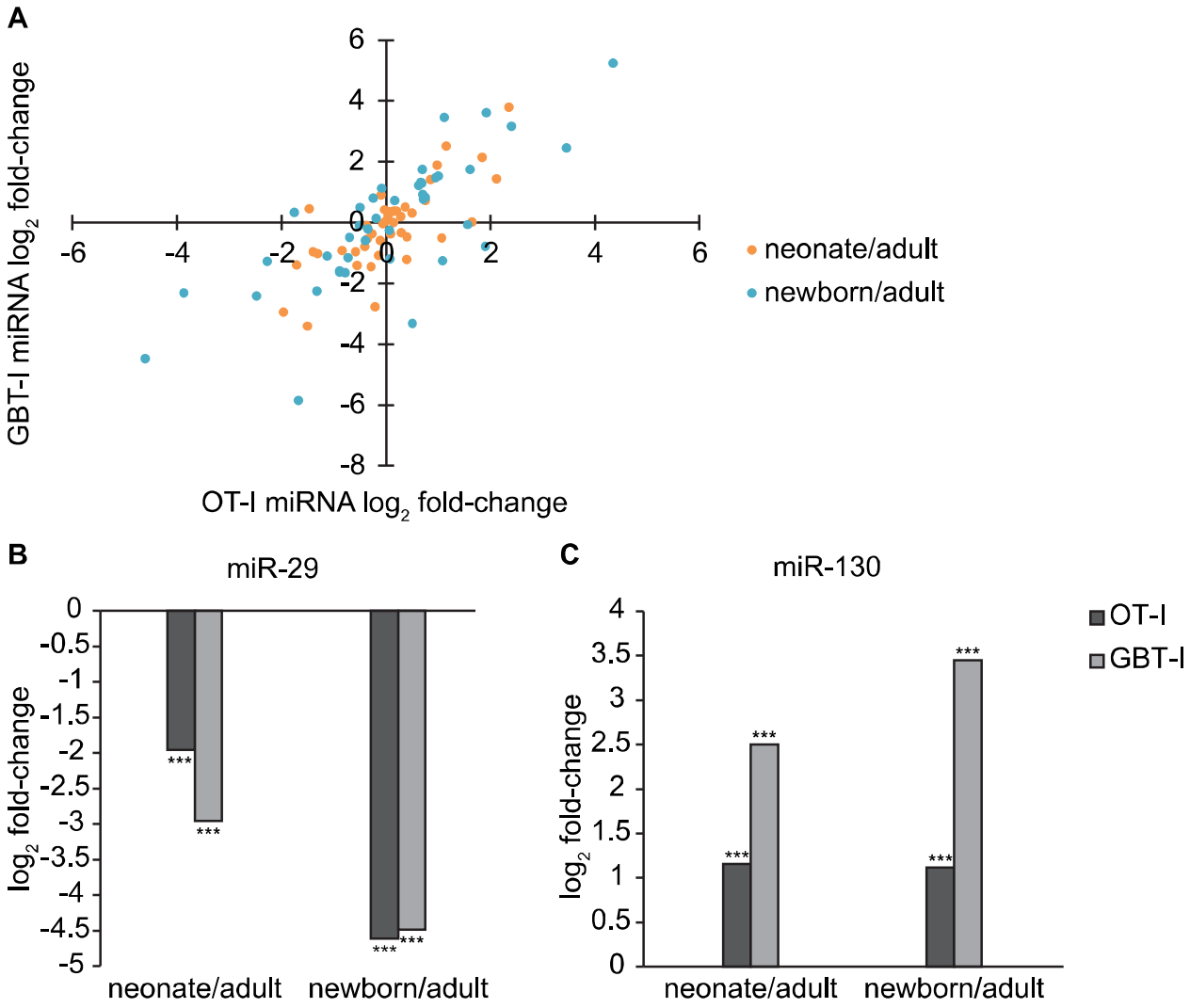

Figure S3 CD8+ T cells from two transgenic TCR mouse strains have similar age-dependent miRNA expression differences. (A) Correlation of fold-changes in neonatal:adult (Pearson r=0.753) and newborn:adult (Pearson r=0.765) miRNA expression between gBT-I and OT-I naive CD8+ T cell biological replicates. Fold-change values were calculated with edgeR; each sample corresponded to two biological replicates, except the gBT-I newborn, which had one. (B) Fold-change in expression of miR-29a between adults and neonates, or adults and newborns, for OT-I and gBT-I naive CD8+ T cells. Differential expression was determined by edgeR; ***=p<0.0005. (C) Fold-change in expression of miR-130b between adults and neonates, or adults and newborns, for OT-I and gBT-I naive CD8+ T cells. Differential expression was determined by edgeR; ***=p<0.0005.

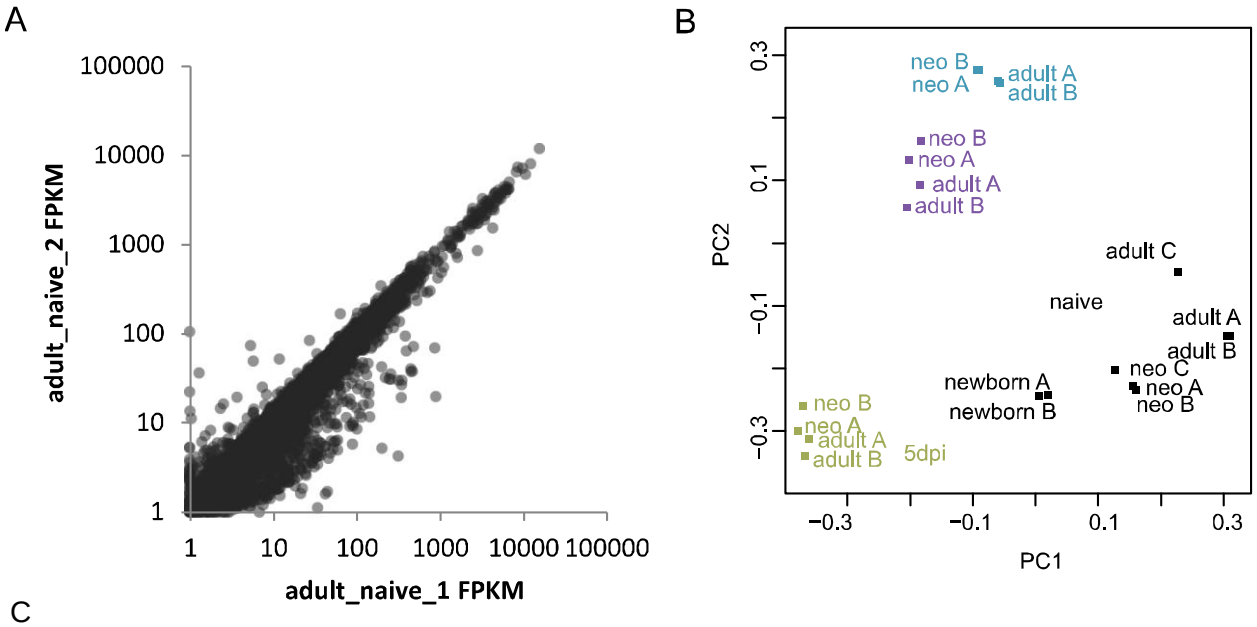

C

Replicate 1	Replicate 2	Pearson R	Pearson p value	Spearman ρ	Spearman p value
adult_naive_0	adult_naive_1	0.99891	$<10^{-15}$	0.99573	$<10^{-15}$
adult_naive_0	adult_naive_2	0.98925	$<10^{-15}$	0.96091	$<10^{-15}$
adult_naive_1	adult_naive_2	0.98826	$<10^{-15}$	0.96041	$<10^{-15}$
adult_5dpi_0	adult_5dpi_1	0.99823	$<10^{-15}$	0.99763	$<10^{-15}$
adult_7dpi_0	adult_7dpi_1	0.99824	$<10^{-15}$	0.99651	$<10^{-15}$
adult_15dpi_0	adult_15dpi_1	0.99954	$<10^{-15}$	0.99823	$<10^{-15}$
neonate_naive_0	neonate_naive_1	0.99769	$<10^{-15}$	0.99009	$<10^{-15}$
neonate_naive_0	neonate_naive_2	0.99408	$<10^{-15}$	0.98841	$<10^{-15}$
neonate_naive_1	neonate_naive_2	0.99207	$<10^{-15}$	0.98722	$<10^{-15}$
neonate_5dpi_0	neonate_5dpi_1	0.99515	$<10^{-15}$	0.9964	$<10^{-15}$
neonate_7dpi_0	neonate_7dpi_1	0.99434	$<10^{-15}$	0.99671	$<10^{-15}$
neonate_15dpi_0	neonate_15dpi_1	0.99891	$<10^{-15}$	0.99785	$<10^{-15}$
newborn_naive_0	newborn_naive_1	0.99870	$<10^{-15}$	0.99558	$<10^{-15}$

Figure S4 mRNA profiles determined by high-throughput sequencing compared between biological replicate samples. (A) Genes that were well-expressed (FPKM>1 in at least one sample) were used; expression values (FPKM) for well-expressed genes (11,360) are shown for two biological replicates. (B) Principal component analysis was performed on all replicate samples for well-expressed genes. (C) Pearson and Spearman correlation coefficients for all pairs of biological replicates that underwent mRNA sequencing.

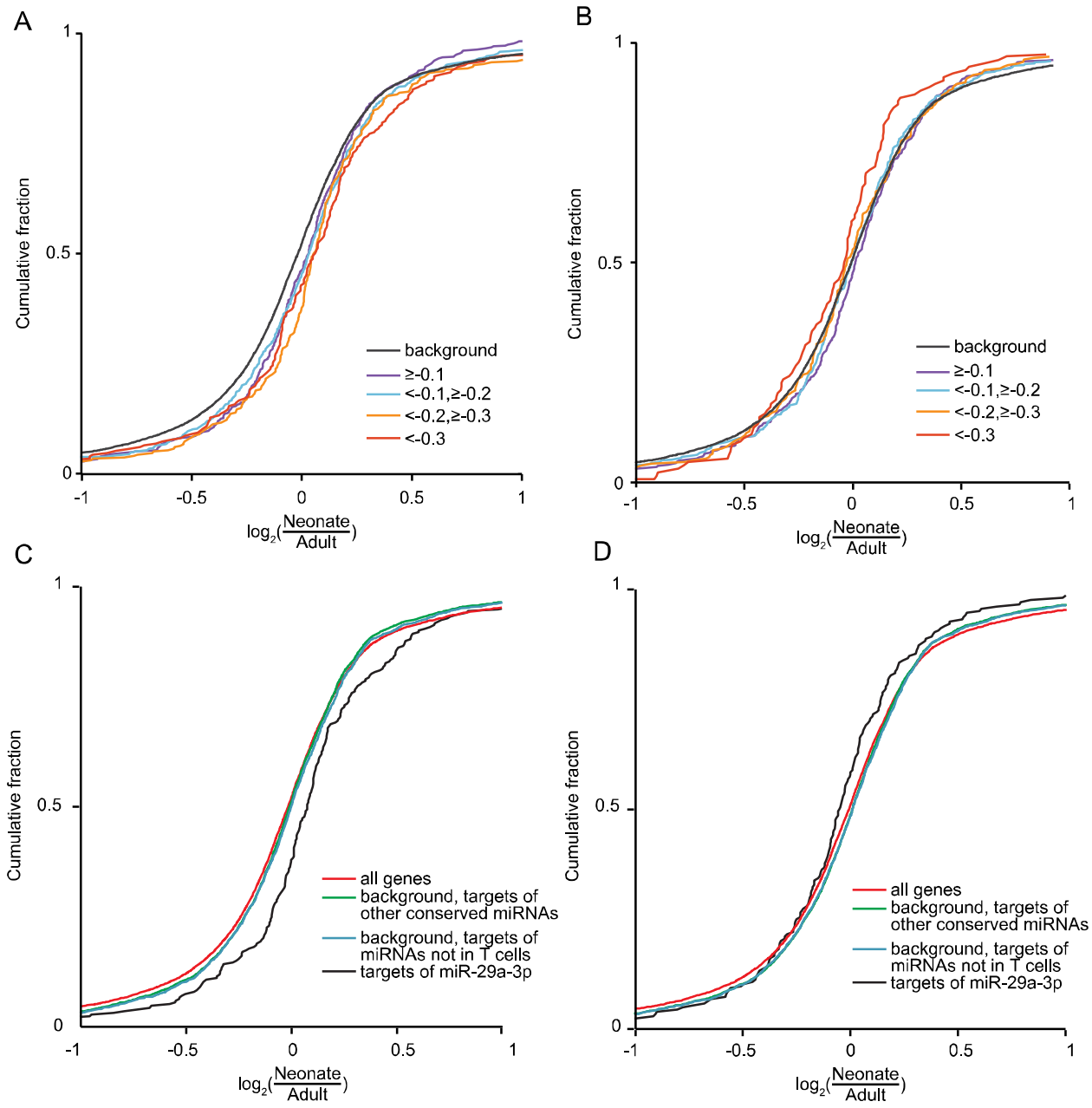

Figure S5 miRNA targeting analysis. (A and B) Targets of miR-29a-3p (A) and miR-130b-3p (B) were binned by context score, regardless of conservation status, to confirm that stronger targets were more repressed by their cognate miRNA than were weaker targets. The background set used was all well-expressed genes, excluding targets for the miRNA being tested. For miR-29a-3p, all context score bins are significantly different from background (context ≥-0.1, $p<0.05$; context <-0.1, ≥-0.2, $p<0.005$; context <-0.2, ≥-0.3, $p<10^{-6}$; context <-0.3, $p<0.05$). For miR-130b-3p, targets with context scores <-0.3 were significantly different from background ($p<0.05$). (C and D) MicroRNA targeting signatures are robust to alternative background gene sets. We tested background sets consisting of all well-expressed genes (red), well-expressed genes that are strong targets of broadly conserved miRNAs (defined in Friedman *et al.* 2009, green), and well-expressed genes that are targets of broadly conserved miRNAs excluding those well-expressed in CD8+ T cells. Compared to all background sets, strong miR-29a-3p targets (C, gray) have significantly different expression ($p<0.0005$). Similarly, strong miR-130b-3p targets (D, gray) have significantly different expression ($p<0.05$) when compared to all different background sets tested.

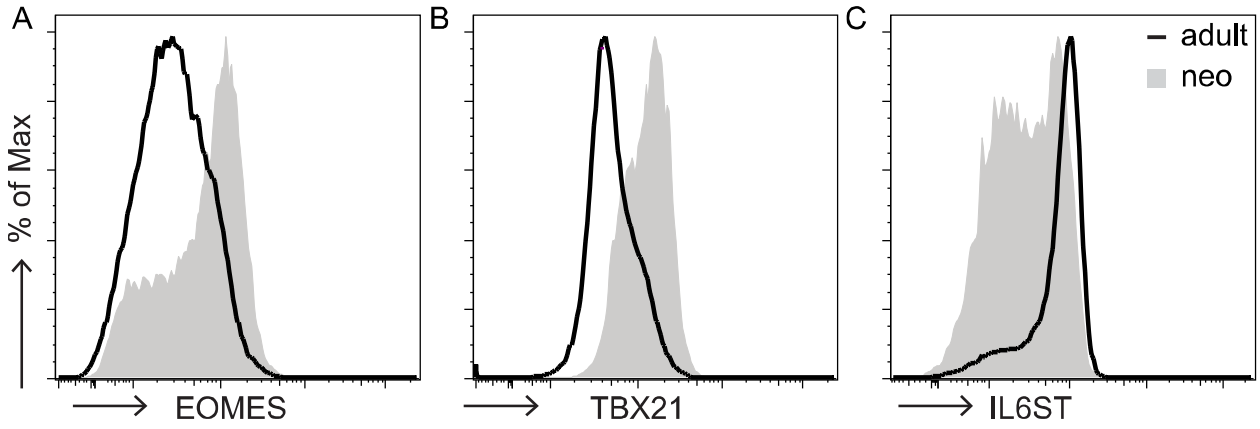

Figure S6 Representative flow cytometry plots. Protein expression in naive adult and neonatal CD8+ T cells of EOMES (A), TBX21 (B), and IL6ST (C) were quantified by flow cytometry.

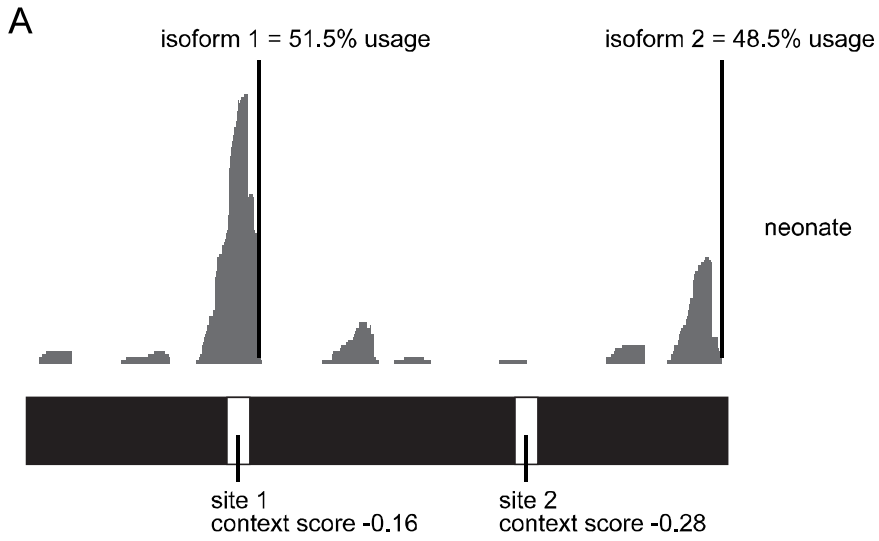

Actual score=(isoform 1 usage x site 1 score) + (isoform 2 usage x site 1 score) + (isoform 2 usage x site 2 score)
Acutal score=(0.515 x -0.16) + (0.485 x -0.16) + (0.485 x -0.28) = -0.29429
Expected score=-0.16-0.28=-0.44

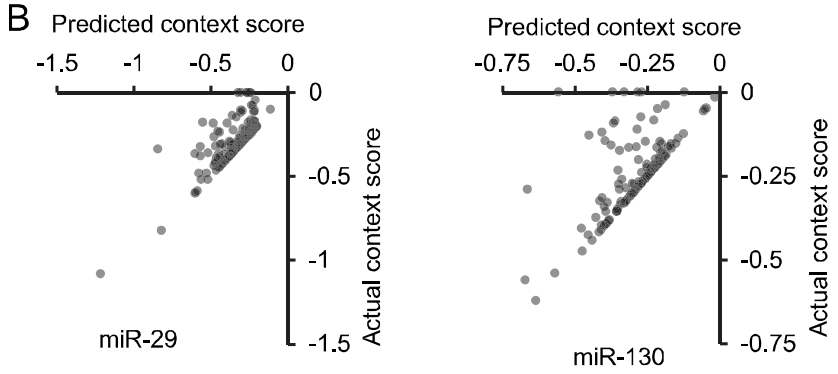

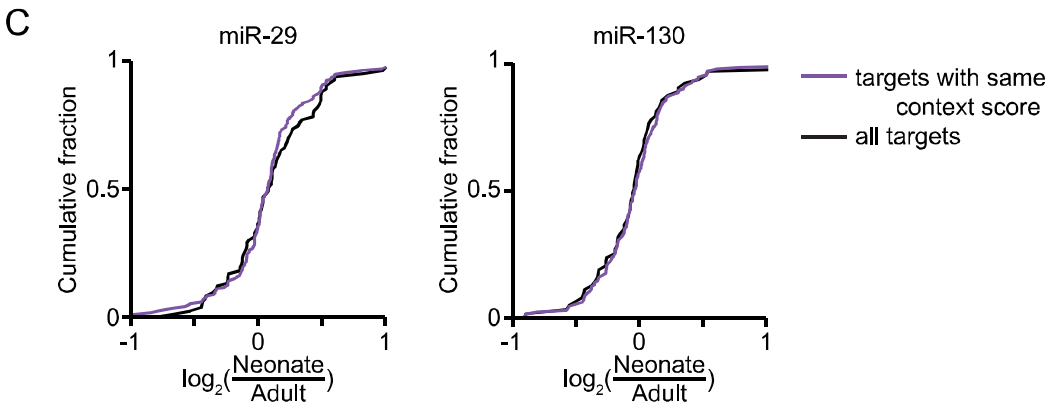

Figure S7 Context scores for isoforms of miRNA targets expressed in CD8+ T cells. (A) Example of calculation of actual context scores using experimentally verified 3'UTR isoforms. For each target, we found expressed isoforms (each isoform consisting of ≥20% of the reads for that gene), then found the context scores for the individual miRNA target sites in all expressed isoforms. We calculated an average context scores of the target sites, weighting them by the usage of that site, as determined by 3'-Seq. *Eomes* has two isoforms and two target sites. One target site is found in both isoforms, whereas the second is found only in the longer isoform. Their scores are weighted based on site usage (51.5% usage for site 1 and 48.5% usage for site 2 in neonates). (B) For each strong predicted target of miR-29a-3p (left) or miR-130b-3p (right), we calculated an actual context score, taking into account the miRNA target sites present. We then compared the average context score for adults and neonates to the expected score (Pearson r=0.789 for miR-29a-3p targets; Pearson r=0.628 for miR-130b-3p targets); high correlations indicate most, but not all, targets have very similar context scores to predicted. (C) We compared the fold-change difference in expression for all predicted targets of miR-29a-3p (left) and miR-130b-3p (right) to fold-change differences for only targets whose experimentally determined isoforms have the predicted context scores. The two groups are not significantly different according to two-sided Kolmogorov–Smirnov tests (miR-29a-3p: p=0.825; miR-130b-3p: p=0.991).

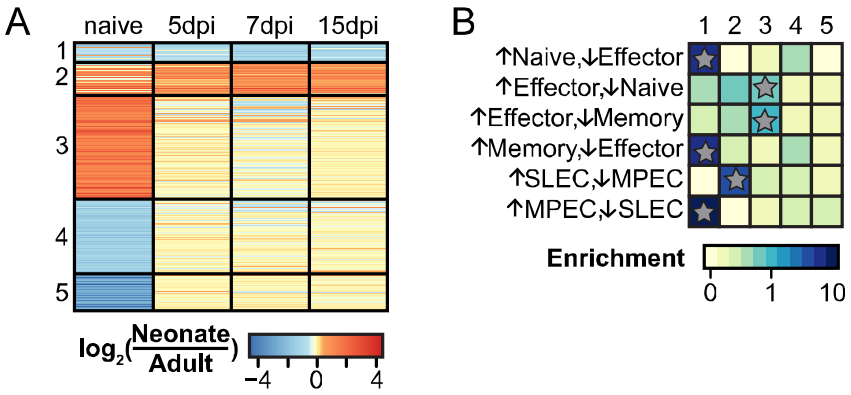

Figure S8 Clustering gene expression differences between adults and neonates. (A) Clustering of co-regulated genes in neonatal and adult CD8+ T cell transcriptomes. Fold-change differences for genes with significant differential expression between adults and neonates were calculated, and fold-differences used to cluster co-regulated groups of genes (as described in Figure 6); see also File S7. (B) Genes in each cluster were compared to genes that define naive, effector, memory cells, MPEC, or SLEC cells. Enrichment was calculated as number of genes in each cluster as compared to the number expected. Significance was determined by Fisher exact tests, *$p<10^{-4}$.

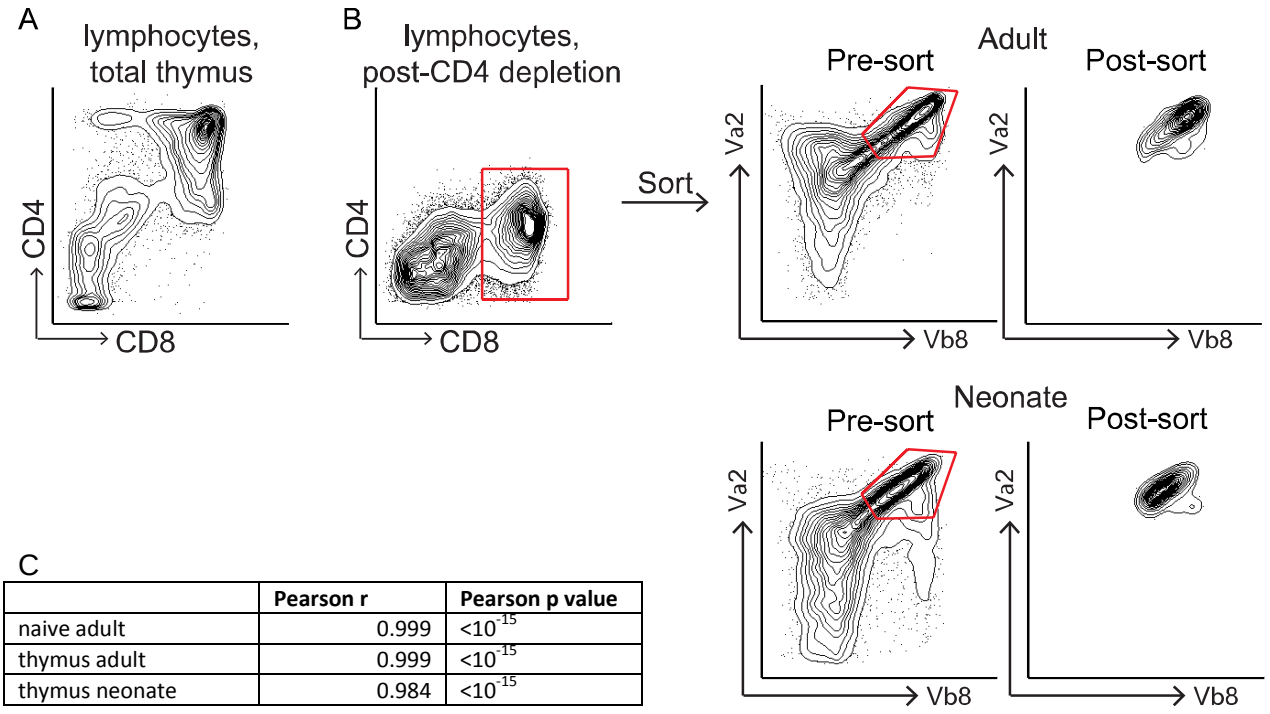

C

	Pearson r	Pearson p value
naive adult	0.999	$<10^{-15}$
thymus adult	0.999	$<10^{-15}$
thymus neonate	0.984	$<10^{-15}$

Figure S9 Thymus cells. (A) Distribution of CD4+ and CD8+ T cells in thymus. (B) Sorting strategy. Thymic cells were depleted of CD4+ cells, then Va2+ Vb8+ cells were FACS sorted to >90% purity. The sorted populations are shown in red boxes. (C) Pearson correlation coefficients for biological replicate miRNA sequencing data.

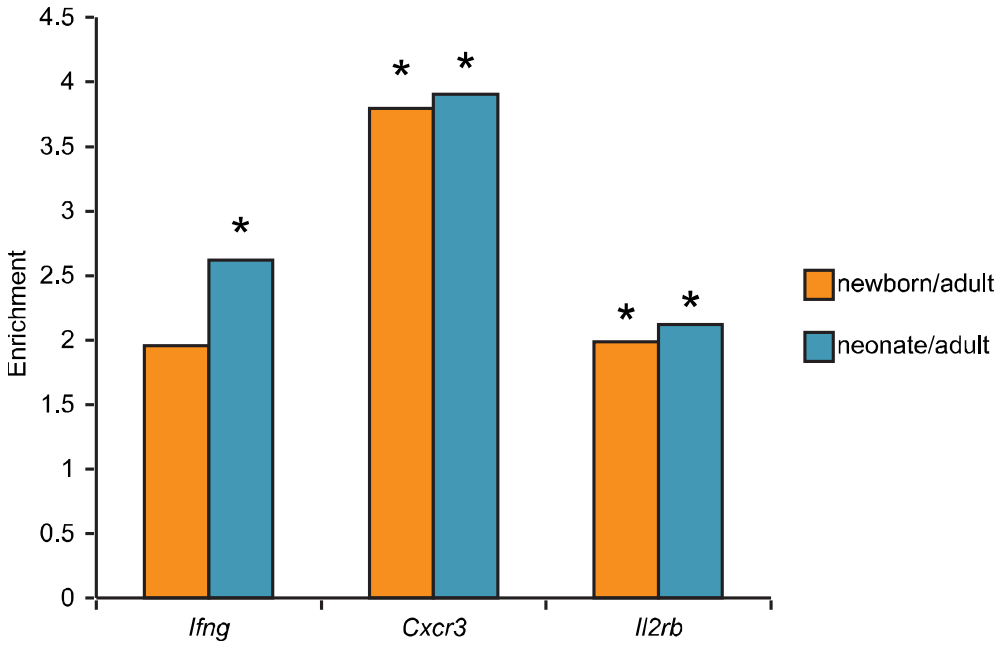

Figure S10 Expression differences for genes regulated by *Tbx21* and *Eomes*. Fold-change differences for genes were calculated between newborn/neonate and adults; *Benjamini-Hochberg corrected p<0.05.

File S1
Supporting Materials and Methods

Preparation of human samples. Whole blood samples from adults and cord blood were obtained from New York Blood Center (Long Island City, NY) and National Disease Research Interchange (Philadelphia, PA), respectively. To isolate mononuclear cells from whole blood, samples were mixed with 1-2 times their volume of PBS-EDTA. This diluted blood was layered over Ficoll-paque Plus (GE Healthcare), then centrifuged at 400g for 30 minutes at room temperature. Mononuclear cells at the interface between plasma and Ficoll were collected and washed with PBS-EDTA. To isolate CD8+ T cells from this fraction, a Naive CD8+ T Cell Isolation Kit (human) (Miltenyi) was used according to manufacturers' instructions. Following isolation, cells were placed in Trizol (Life Technologies).

Mice. gBT-I TCR transgenic mice (TCRαβ specific for SSIEFARL peptide from HSV-1 glycoprotein B498-505) were provided by Dr. Janko Nikolich-Zugich (University of Arizona, Tucson, AZ). Ly5.2 mice (8-12 wk) were purchase from The National Cancer Institute (Fredrick, MD). Rag-/- OT-I mice were purchased from Taconic (Germantown, NY) and were crossed to C57Bl/6 mice from The National Cancer Institute and F1 progeny were used.

Antibodies, Staining and Flow Cytometry. The fluorochrome labeled monoclonal antibodies anti-CD8α (53-6.7), anti-CD4 (GK1.5), anti-CD45.1 (A20), anti-CD45.2 (104), anti-CD90.1/Thy1.1 (OX-7), anti-KLRG1 (2F1), anti-CD127 (A7R34), anti-CD62L (MEL-14), anti-CD44 (clone), anti-Eomes (Dan11mag), anti-T-bet (eBio4B10), anti-CXCR3 (CXCR3-173), anti-CCR5 (HM-CCR5), anti-CCR7 (4B12) and anti-gp130 (KGP130) were purchased from Biolegend (San Diego, CA), eBioscience (San Diego, CA), Life technologies (Carlsbad, CA) or BD Biosciences (San Jose, CA).

Sorting. Splenocytes were harvested and positive magnetic selection was performed using anti-CD8 beads (Miltenyi Biotec, Auburn, CA), according to manufacturer's instructions. Following purification, cells were labeled with anti-CD4-fluorescein isothiocyanate, anti-CD8-e450, anti-Thy1.1-allophycocyanin, anti-CD45.2,-allophcyocyanin-e780 and anti-CD45.1-phycoerythrin-Cy7 for 30 min at 4°C. Labeled cells were washed twice and placed in sorting buffer (PBS, 0.5% BSA, 2 mM EDTA). We concurrently sorted for CD8+CD4-CD45.1-CD45.2+Thy1.1+ and CD8+CD4-CD45.1-CD45.2+Thy1.1- populations and achieved >95% purity. Sorting was performed on a FACS Aria (BD Biosciences).

RNA isolation. Cells were resuspended in Trizol (Life Technologies) at a concentration of 1 million cells/mL and stored at -80°C. RNA isolation was completed within a month. To do so, the samples were thawed and 200 µL of chloroform per mL Trizol was added. The tubes were shook for 15 seconds, then incubated at room temperature for ten minutes to allow for phase

separation. The tubes were centrifuged for 15 minutes at 12,000xg at 4°C. The upper aqueous phase was transferred to a fresh tube, and 1 µL glycoblue (Life Technologies) was added to help visualize the RNA pellet. To precipitate the RNA, we added 0.5 mL isopropanol per mL Trizol, then incubated at room temperature for ten minutes, then centrifuged for ten minutes at 12,000xg at 4°C. The supernatant was pipetted off, and the pellet was washed in 1 mL 75% ethanol, then centrifuged for ten minutes at 12,000xg at 4°C. The supernatant was pipetted off and the RNA pellet was allowed to air dry for ten minutes. The RNA was then resuspended in 20 µL RNase-free water (HyClone).

Small RNA-Seq analysis. We used miRDeep2 to align and quantify sequencing reads to known mouse miRNAs (Friedländer *et al.* 2012). For aligning, we inputted the raw sequencing files into the script mapper.pl (a component of miRDeep2) which trimmed the adapter sequence (TGGAATTCTCGGGTGCCAAGG for libraries generated with Illumina, AGATCGGAAGAGCACACGTCT for libraries generated with NEB), discarded reads with fewer than 18 nucleotides, aligned the reads to the genome (mm9) using Bowtie (Langmead *et al.* 2009). We used options –e, -h, -i, -j, -k, -l 18, and -m.

Genome-matching reads were matched to known mouse miRNAs from miRBase version 21 (Kozomara and Griffiths-Jones 2014) and quantified using the script quantifier.pl (a component of miRDeep2) using options –d and –t mmu. The defaults we used allow one mismatch and allow 2 nucleotides upstream and 5 nucleotides downstream of the mature sequence.

For each miRNA, we normalized the number of reads in each sample by the total number of miRNA-matching reads, then found all miRNAs with >1000 RPM (well-expressed) in at least one sample. We then combined those miRNAs that come from the same miRNA family, as defined by having the same composition at nucleotides 2-8. We used the raw read counts for those miRNA families when finding fold-change differences and differential expression using edgeR (Robinson *et al.* 2010). When using edgeR, we calculated normalization factors, estimated common and tagwise dispersion, and performed exact tests on each adult and neonatal pair for naïve, 5-dpi, and 7-dpi samples. The p-values are multiple test corrected using the Benjamini-Hochberg method.

Clustering was performed using the Euclidean method in the R package gplots. Principal component analysis was performed on $\log_{10}$(RPM) values for the miRNAs with >1000 RPM in at least one sample.

mRNA-Seq analysis. We trimmed nucleotides from the ends of sequencing reads if they had Phred quality scores <20. Reads that were at least 20 nucleotides long after trimming were aligned to the genome (mm9) using Tophat (Trapnell *et al.* 2009) with the option --no-novel-juncs. We used the mm9 GTF file provided by UCSC (available from the Tophat website). Differential expression of genes between samples was determined using CuffDiff (Trapnell *et al.* 2013) with a false discovery rate of 5%.

Clustering gene expression data. We clustered expressed genes that were significantly differentially expressed, and had at least a 2-fold difference in expression between adults and neonates in at least one sample (naïve, 5-dpi, 7-dpi, or 15-dpi). Those genes were grouped into five clusters using the partioning around medoids method (Reynolds *et al.* 2006) in R.

Enrichment statistics. Gene sets were downloaded from the Immunologic Signatures collection at the Molecular Signatures Database (MSDB). We found the number of genes from each dataset that belonged to a cluster. For each cluster, we found the number of genes that were found in both the cluster and the dataset (b), the total number of genes present in that cluster (n), the number of genes in the MSDB dataset (B), and the total number of genes that had been clustered (N). Enrichment was calculated as $\frac{b/n}{B/N}$. One-sided Fisher exact tests were used to measure significance.

3'-Seq. 3'-Seq was performed as described in (Lianoglou *et al.* 2013) (full protocol available at http://www.mskcc.org/sites/www.mskcc.org/files/node/25002/documents/3%27-seq%20protocol.pdf). Briefly, 1 ug of DNase-treated (Ambion) total RNA was incubated with a biotinylated polyT primer that contained a single RNA base (IDT) and Dynabeads M280 Steptavidin (Life Technologies). The RNA attached to the beads underwent first strand synthesis with SuperScriptIII (Life Technologies), then second strand synthesis with DNA Pol I (NEB) and RNaseH (NEB). The cDNA was nicked using RNase HII to introduce then translated with DNA Pol I (NEB) for 8 minutes at 8°C. After stopping the reaction with EDTA at 50 mM, the ends were cleaned up with T7 exonuclease (NEB), mung bean exonuclease (NEB), and Klenow enzyme (NEB) supplemented with dNTPs. Adapters were ligated with T4 DNA ligase (NEB), then amplified with Phusion (Fermentas). After the libraries were purified by PAGE, they were sequenced on the Hi-Seq platform with 100 bp reads.

3'-Seq analysis. To ensure that we were examining reads that captured the ends of 3'UTRs, we required that 3'-Seq reads contain the 3' adapter sequence adjacent to a stretch of A's. We then trimmed the A's and the adapter sequence from the 3' end of the read, then trimmed low quality nucleotides (Phred <20) from the 5' and 3' end of the read. Trimmed reads that were at least 20 nucleotides long, and were not derived from rRNA (removed using local alignment Bowtie2)Langmead *et al.* 2009; Langmead and Salzberg 2012), were then mapped to the mouse genome (mm9) using Tophat. The 3' end of uniquely matching reads were mapped and counted using the Genomecov tool from Bedtools (Quinlan and Hall 2010). We kept reads that mapped either in an annotated mouse 3'UTR (RefSeq, mm9) or within 1500 nt downstream, and we only considered the longest annotated 3'UTR isoform for genes that are reported to have multiple isoforms. We then determined which reads were within 50 nucleotides of a putative polyadenylation sequence (PAS, AATAAA or ATTAAA), and used those in further analyses. For each gene, an isoform was considered if it contained at least 20% of the reads for that gene. For genes that were targets of miR-29a-3p or miR-130b-3p and that did not end at the annotated position, we used TargetScan Mouse release 6.2 (Friedman

et al. 2009; Garcia *et al.* 2011)to determine if any miRNA target sites were lost in the shorter isoforms, using information from the files Conserved site context+ scores.txt and Nonconserved site context+ scores.txt.

Cloning. We used nested PCR to amplify fragments of 3'UTRs from genomic mouse DNA (Promega). The PCR primers were flanked with a SacI site on the forward oligo and a NotI site on the reverse oligo. We digested the PCR products and pmirGlo (Promega) with SacI-HF and NotI-HF (NEB), then ligated them with T4 DNA Ligase (NEB). We used site-directed mutagenesis (Agilent) to mutate the miRNA target sites at two positions. Our oligo sequences are:

Eomes	Outer PCR, forward	AACTAAACTGAAGCAGACCTAGCA
Eomes	Outer PCR, reverse	TGACCAAGGAAAGAGGATTAAGCA
Eomes	Inner PCR, forward	ATATATGAGCTCATGGGAAACGAGAAATGTTCAGAA
Eomes	Inner PCR, reverse	ATATATGCGGCCGCCGAAGTGGACAGAATATCTCCAAG
Tbx21	Outer PCR, forward	AGGTGCCCACTAACTTAGAAAACA
Tbx21	Outer PCR, reverse	ACCAGGTCCATGTTTATTTCCAGA
Tbx21	Inner PCR, forward	ATATATGAGCTCGGATTCTGGGGTTTACTTCTTGTT
Tbx21	Inner PCR, reverse	ATATATGCGGCCGCCCAGAAAGTGATGCAAAACAGAAG
Bak1	Outer PCR, forward	CCTGGCTGGACTAAACCTCTCT
Bak1	Outer PCR, reverse	TGAAGGTGGGGTTCAAGTAATCAT
Bak1	Inner PCR, forward	ATATATGAGCTCCTGGACTAAACCTCTCTCCCTAC
Bak1	Inner PCR, reverse	ATATATGCGGCCGCATGGATGGATTGGGGTAGGAGATA
Cd69	Outer PCR, forward	CACCACAGGAAAGTTGTGTAACTG
Cd69	Outer PCR, reverse	AACAGGTTATGTGACAAGACTGGA
Cd69	Inner PCR, forward	ATATATGAGCTCGACTGCACAAACCAACTTTACATC
Cd69	Inner PCR, reverse	ATATATGCGGCCGCCCTTGAAATACGCTACAGAGGTTT
Irf1	Outer PCR, forward	CTTGACACATGGCAAAGCATAGTC
Irf1	Outer PCR, reverse	CATGACCAAACACCATTTAGCAGT
Irf1	Inner PCR, forward	ATATATGAGCTCTCTGAGTTTTCTTGTGAGGTGAAG
Irf1	Inner PCR, reverse	ATATATGCGGCCGCATAGATAGTCAAGAGTCACGCCAA
Il6st	Outer PCR, forward	TAAAGACGAGTGGCTTCAGATGAG
Il6st	Outer PCR, reverse	CTGTAGGAGGACTTCTGTCATTGT
Il6st	Inner PCR, forward	ATATATGAGCTCCTTCAGATGAGAAACAGTCCTCAC

Il6st	Inner PCR, reverse	ATATATGCGGCCGCATAATAAGCAGTTTCTTGGGAGGC
Eomes upstream	Mutagenize miR-29 site, F	GCTATGAAGAACGAGTGCCCGGTACCATTAAATGAATTTCAAAG
Eomes downstream	Mutagenize miR-29 site, F	GGTATCAGATAAAAATAATGTAAATTTGGTACCTTGGCGTTGTAAAGAATTTGC
Tbx21	Mutagenize miR-29 site, F	CAGTCACGAACCTGGTACCGCTTCTGACCCC
Tbx21	Mutagenize miR-29 site, R	GGGGTCAGAAGCGGTACCAGGTTCGTGACTG
Bak1	Mutagenize miR-29 site, F	CCCCAACATTGCATGGTACCACTGAACCCCATCC
Bak1	Mutagenize miR-29 site, R	GGATGGGGTTCAGTGGTACCATGCAATGTTGGGG
Cd69	Mutagenize miR-130 site, F	CCAGTGCCTTTACGCATTAGCGCTATTTGGAGGGGTTTC
Cd69	Mutagenize miR-130 site, R	GAAACCCCTCCAAATAGCGCTAATGCGTAAAGGCACTGG
Irf1	Mutagenize miR-130 site, F	CTCTGTACTAGGAGACAATAGCGCTAAATGAGTCCTATTCCC
Irf1	Mutagenize miR-130 site, R	GGGAATAGGACTCATTTAGCGCTATTGTCTCCTAGTACAGAG
Il6st	Mutagenize miR-130 site, F	GTGCTCTTTCAGAATGTTAGCGCTGCCGAAAACAAAGTGTGTC
Il6st	Mutagenize miR-130 site, R	GACACACTTTGTTTTCGGCAGCGCTAACATTCTGAAAGAGCAC

Cell culture. HEK293 cells were used because they express negligible amounts of miR-29 and no detectable miR-130 (Mayr and Bartel 2009). They were maintained in DMEM (Gibco) supplemented with 10% FBS and penicillin/streptomycin at 37°C with 5% CO_2. At 24-hours before transfection, we plated cells at 50,000 cells/mL in 24-well plates. We transfected 10 ng of the experimental plasmid and 25 nmol of miRNA mimic (IDT) using Lipofectamine 2000 (Life Technologies). We harvested the cells 24 hours later and stored them at -80°C. Luciferase amounts for Firefly and *Renilla* were measured using the Dual-Luciferase Reporter Assay system (Promega) with a dual-injection luminometer (Turner Biosystems). Firefly luciferase luciferase levels were normalized to *Renilla*. The miRNA mimic sequences are:

miR-29 sense strand	UAGCACCAUCUGAAAUCGGUUA
miR-29 anti-sense strand	ACCGAUUUCAGAUGGUGUUAAU
miR-130 sense strand	CAGUGCAAUGUUAAAAGGGCAU
miR-130 anti-sense strand	GCCCUUUUAACAUUGCACAGAU

Files S2-S7

Available for download at www.genetics.org/lookup/suppl/doi:10.1534/genetics.115.179176/-/DC1

File S2 Expression values (reads per million) for miRNAs that are well-expressed in at least one sample.

File S3 Fold-change expression changes between adults, neonates, and newborns for miRNA families.

File S4 Gene expression of miRNA targets.

File S5 Positions and expression of 3'UTR isoforms.

File S6 Expression and differential expression information for expressed genes.

File S7 Genes present in clusters.

Literature Cited

Friedländer M. R., Mackowiak S. D., Li N., Chen W., Rajewsky N., 2012 miRDeep2 accurately identifies known and hundreds of novel microRNA genes in seven animal clades. Nucleic Acids Res. **40**: 37–52.

Friedman R. C., Farh K. K.-H., Burge C. B., Bartel D. P., 2009 Most mammalian mRNAs are conserved targets of microRNAs. Genome Res. **19**: 92–105.

Garcia D. M., Baek D., Shin C., Bell G. W., Grimson A., Bartel D. P., 2011 Weak seed-pairing stability and high target-site abundance decrease the proficiency of lsy-6 and other microRNAs. Nat. Struct. Mol. Biol. **18**: 1139–1146.

Kozomara A., Griffiths-Jones S., 2014 miRBase: annotating high confidence microRNAs using deep sequencing data. Nucleic Acids Res. **42**: D68–D73.

Langmead B., Trapnell C., Pop M., Salzberg S. L., 2009 Ultrafast and memory-efficient alignment of short DNA sequences to the human genome. Genome Biol. **10**: R25.

Langmead B., Salzberg S. L., 2012 Fast gapped-read alignment with Bowtie 2. Nat. Methods **9**: 357–359.

Lewis B. P., Burge C. B., Bartel D. P., 2005 Conserved Seed Pairing, Often Flanked by Adenosines, Indicates that Thousands of Human Genes are MicroRNA Targets. Cell **120**: 15–20.

Lianoglou S., Garg V., Yang J. L., Leslie C. S., Mayr C., 2013 Ubiquitously transcribed genes use alternative polyadenylation to achieve tissue-specific expression. Genes Dev. **27**: 2380–2396.

Mayr C., Bartel D. P., 2009 Widespread shortening of 3'UTRs by alternative cleavage and polyadenylation activates oncogenes in cancer cells. Cell **138**: 673–684.

Quinlan A. R., Hall I. M., 2010 BEDTools: a flexible suite of utilities for comparing genomic features. Bioinformatics **26**: 841–842.

Reynolds A. P., Richards G., Iglesia B. de la, Rayward-Smith V. J., 2006 Clustering Rules: A Comparison of Partitioning and Hierarchical Clustering Algorithms. J. Math. Model. Algorithms **5**: 475–504.

Robinson M. D., McCarthy D. J., Smyth G. K., 2010 edgeR: a Bioconductor package for differential expression analysis of digital gene expression data. Bioinforma. Oxf. Engl. **26**: 139–140.

Trapnell C., Pachter L., Salzberg S. L., 2009 TopHat: discovering splice junctions with RNA-Seq. Bioinformatics **25**: 1105–1111.

Trapnell C., Hendrickson D. G., Sauvageau M., Goff L., Rinn J. L., Pachter L., 2013 Differential analysis of gene regulation at transcript resolution with RNA-seq. Nat. Biotechnol. **31**: 46–53.